BOLETIN DE LA SOCIEDAD ESPAÑOLA DE
Cerámica y Vidrio
www.elsevier.es/bsecv

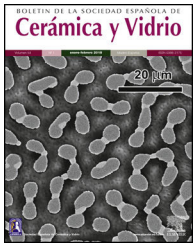

Assessment of nickel oxide substituted bioactive glass-ceramic on in vitro bioactivity and mechanical properties

Vikash Kumar Vyas[a,*], *Arepalli Sampath Kumar*[a], *Akher Ali*[a], *Sunil Prasad*[a], *Pradeep Srivastava*[b], *Sarada Prasanna Mallick*[b], *Md Ershad*[a], *Saryoo Prasad Singh*[a], *Ram Pyare*[a]

[a] *Department of Ceramic Engineering, Indian Institute of Technology, Banaras Hindu University, Varanasi 221005, India*
[b] *School of Biochemical Engineering, Indian Institute of Technology, Banaras Hindu University, Varanasi 221005, India*

ARTICLE INFO

Article history:
Received 18 May 2016
Accepted 25 September 2016
Available online 1 November 2016

Keywords:
Bioactive glasses
Bioactive glass ceramics
Mechanical properties
Nickel oxide
FTIR spectrometry and cell culture

ABSTRACT

Many type of oxide substituted glass-ceramics like strontium, cobalt, barium and titanium have shown bioactivity with improved mechanical properties. The present work reports the in vitro bioactivity and mechanical properties of nickel oxide substituted in bioactive glass-ceramic and results were compared with 45S5 bioactive glass-ceramic. Bioactive glass ceramics were processed through controlled crystallization of their respective bioactive glasses. The formed crystalline phases in bioactive glass-ceramics were identified using X-ray diffraction (XRD) analysis. The formation of HA layer was assessed by immersing them in the simulated body fluid (SBF) for different soaking periods. The formation of hydroxyapatite was confirmed by FTIR spectrometry, SEM and pH measurement. Densities and mechanical properties of the samples were found to increase considerably with an increasing the concentration of nickel oxide. A decrease in glass transition temperature (Tg) with NiO addition showed that the nickel oxide had acted as an intermediate in smaller quantities in the bioactive glass. The cell culture studies demonstrated that the samples containing low concentration of NiO from 0 to 1.65 mol% were non-cytotoxic against osteoblast cells. Finally, this investigation clearly concluded that NiO doped bioactive glass would be potential biomaterials for biomedical applications.

Evaluación del efecto de la sustitución de SiO_2 por NiO sobre la bioactividad y las propiedades mecánicas de vitrocerámico bioactivos

Palabras clave:
Vidrios bioactivos
Bioactivos-vidrio-cerámica
Propiedades mecánicas
Óxido de níquel

RESUMEN

La sustitución de óxidos en la composición de vitrocerámicos bioactivos por otros como son los de estroncio, cobalto, barrio y titanio han demostrado bioactividad con una mejora de sus propiedades mecánicas. En el presente trabajo se muestra el efecto de la sustitución de SiO_2 por NiO, en vitrocerámicos basados en la composición del biovidrio 45S5, sobre la bioactividad y las propiedades mecánicas, comparándose los resultados obtenidos. Los

* *Corresponding author.*
E-mail address: vkvyas.rs.cer11@itbhu.ac.in (V.K. Vyas).
http://dx.doi.org/10.1016/j.bsecv.2016.09.005

Espectrometría FTIR y célula de la cultura

vitrocerámicos se obtuvieron mediante cristalización controlada de los respectivos biovidrios. Las fases cristalizadas se identificaron mediante Difracción de Rayos X (DRX). La formación de una capa de hidroxiapatita se evaluó mediante inmersión, durante varios periodos de tiempo, en Suero Fisiológico Artificial (SFA). La formación de dicha capa se confirmó mediante Espectroscopia Infrarroja con Transformada de Fourier (FTIR), Microscopía Electrónica de Barrido (SEM) y medidas de pH. Tanto la densidad como las propiedades mecánicas de las muestras aumentan al aumentar la concentración de NiO, a la vez que se produce una disminución de la temperatura de transición vítrea (Tg). Estudios en cultivos celulares con células osteoblásticas demostraron que las muestras que contienen baja concentración de NiO (0 a 1,65%) en moles no son citotóxicas. Por último, esta investigación concluye claramente que estos biovidrios dopados con NiO son potenciales biomateriales para aplicaciones biomédicas.

Introduction

Bioactive glasses used in biomedical application must have the ability to form chemical bond with bones and help in new bone growth [1,2]. Traditional melting method is considered as simple and suitable for mass production [3,4]. Hench and his team had invented first bioactive glass named as 45S5 bioglass® [5]. The bioactivity of the 45S5 bioglass® is mainly due to its composition which consists of low SiO_2 (glass network former) content, high CaO/P_2O_5 ratio and high Na_2O and CaO (glass network modifier) contents [6]. Bioactive material should possess good biochemical behavior and biomechanical strength. The 45S5® bioactive glass has very good capability to bond with both the soft and hard tissues [7]. However, poor mechanical properties like brittleness are the main disadvantage of 45S5® bioactive glass. A lot of researches have been carried out for preparation and characterization of bioactive glass and bioceramics with incorporation of some oxides such as CoO, ZnO, NiO and Fe_2O_3 in glasses which changed their mechanical, physical, chemical and bioactive properties [8–10]. The significant effects of oxide doped bioactive glass are on osteoblastic cell proliferation, differentiation and thus bone mineralization [11–14]. Another studies showed that substitution of B_2O_3, MgO, CaF_2 or TiO_2 in phosphate glasses and its ceramic derivatives had also shown bioactivity [15,16]. Substitution of bioactive glasses with different transition metals such as copper, zinc, manganese, iron, magnesium and silver to change their biological and bioactive response has been studied by a number of research groups [17–21]. Medical application of glass-ceramics is limited due to their inherent properties such as brittleness, low tensile strength and difficulty in coating onto other materials [22,23]. Hoppe et al. [24] investigated cobalt oxide releasing 1393 bioactive glass derivative scaffolds for bone tissue engineering applications as cobalt was known as angiogenesis agent. Smith et al. [25] studied the structural characterization of hypoxia-mimicking 45S5 glass prepared with 4.0 mole% of CoO and NiO. They found that bioactive glass containing NiO had offered an existing route for potential delivery system of Ni^{2+} ions with tissue regeneration scaffolds due to its ability to incorporate a large variety of elements such as Ca, P and their appreciably controlled dissolution properties within physiological fluids. It has been also reported earlier that up to 4.0 mole% NiO incorporated into bioglass® has proved physiologically to be appropriate concentrations [26,27] but the cell culture studies have revealed that low concentration NiO doped bioactive glasses are non-cytotoxic against osteoblast cells and suitable for biomedical applications.

The primary aim of the present study is to develop nickel oxide substituted glass-ceramic using the traditional melting method by incorporating varying amount of nickel oxide and study the effect doping of nickel oxide in silica-based bioactive glasses in order to determine its bioactivity and mechanical behavior.

Material and methods

Glass-ceramic preparation

The compositions of bioactive glass-ceramic as given in Table 1, were prepared by substitution of nickel oxide (0–1.65 mol%) in place of SiO_2 using the normal melting and annealing technique. Materials used include fine-grained quartz for silica. Lime and soda were introduced in the form of their respective anhydrous carbonates. P_2O_5 was supplementary in the form of diammonium hydrogen phosphate. The weighed batches were mixed thoroughly for 40 min and melted in alumina crucibles. The melting was carried out in an electric furnace at 1400 ± 5 °C for 3 h in air as furnace atmosphere and homogenized melts were poured on preheated aluminum sheet. The prepared bioactive glass samples were directly transferred to a regulated muffle furnace at 480 °C for annealing. After 2 h of annealing the muffle furnace was cooled to room temperature with controlled rate of cooling at 10 °C/min. Nickel oxide substituted bioactive glass and base

Table 1 – Composition of bioactive glass-ceramics (mol%).

Sample	SiO_2	Na_2O	CaO	P_2O_5	NiO
45S5C	46.14	24.40	26.91	2.55	0.00
NiO-1C	45.64	24.41	26.94	2.60	0.41
NiO-2C	45.20	24.44	26.96	2.61	0.82
NiO-3C	44.71	24.46	26.98	2.61	1.23
NiO-4C	44.25	24.49	27.01	2.61	1.65

Table 2 – Ion concentration (mM/l) of simulated body fluid and human blood plasma.

Ion	Na^+	K^+	Mg^{2+}	Ca^{2+}	HCO_3^-	HPO_4^{2-}	SO_4^{2-}	Cl^-
Simulated body fluid	142.0	5.0	1.5	2.5	4.2	1.0	0.5	147.8
Human blood plasma	140.0	5.0	1.5	2.5	27.0	1.0	0.5	103.0

glass was subjected to differential thermal analysis (DTA) in order to determine glass nucleation and crystallization temperature. Fine powder of bioactive glasses was made using an agate mortar and pestle and analyzed using a differential thermal analyzer (Perkin Elmer Diamond, USA) at a heating rate of 10 °C/min under a stream of argon atmosphere using alumina as a reference material. DTA was carried out from 300 °C to 900 °C temperature.

The prepared bioactive glass samples were heat-treated in two-step system, firstly nucleation temperature for the formation of nuclei sites and after holding for the specific time, it was then further heated to reach the second selected crystal growth temperature. The samples were cooled to room temperature inside the muffle furnace at controlled cooling rate of 10 °C per min.

Preparation of SBF

Kokubo and his colleagues developed simulated body fluid that has inorganic ion concentrations similar to those of human body fluid in order to reproduce in vitro formation of apatite on bioactive materials [28]. The SBF solution was prepared by dissolving reagent-grade NaCl, KCl, $NaHCO_3$, $MgCl_2{\cdot}6H_2O$, $CaCl_2$ and KH_2PO_4 into double distilled water and it was buffered at pH = 7.4 with TRIS (trishydroxymethyl amino methane) and 1 N HCl at 37 °C as compared to human blood plasma (WBC). The ion concentrations of SBF in mM/liter of solution are given in Table 2 [28].

X-ray diffraction analysis of powders

In order to identity the crystalline phase present in the heat-treated bioactive glasses, the samples were ground to 75 μm and the fine powders were subjected to X-ray diffraction analysis (XRD) using RIGAKU-Miniflex II diffractometer adopted Cu-Kα radiation (λ = 1.5405 Å) with a tube voltage of 40 kV and current of 35 mA in a 2θ range between 20° and 80°. The step size and measuring speed was set to 0.02° and 1° per min, respectively was used in the present investigation. The JCPDS-International Center for diffraction Data Cards were used as a reference.

In vitro test of glass-ceramic by FTIR reflectance spectrometry

The structure of glass-ceramic was measured at room in the frequency range of 4000–400 cm^{-1} using a Fourier transform infrared spectrometer (Bruker Tensor 27 FTIR, Germany). The fine glass-ceramic powder samples were mixed with KBr in the ratio of 1:100 and the mixtures were subjected to an evocable die at load of 10 tons/cm^2 to produce clear homogeneous discs. The prepared discs were immediately subjected to FTIR spectrometer to measure the reflection spectra in order to avoid moisture attack. In order to investigate the formation of (calcium phosphate) apatite layer on the surface of the samples after immersion in SBF solution. 2.0 g of the sample was immersed in 20 ml of SBF solution in a small plastic container at 37 °C at the pH of 7.40 in an incubator at static condition for time periods 1, 3, 7, 15 and 30 days. After soaking, the samples were filtered, rinsed with doubly distilled water and dried in an oven at 120 °C for 2 h before FTIR spectrometric analysis.

Mechanical properties and density measurements

The melts were casted in rectangular shape mold and the resultant glass-ceramic samples were ground and polished for required dimension using grinding machine and then samples were subjected to three point bending test. The test was performed at room temperature using Instron Universal Testing Machine (AGS 10kND, SHIMADZU) of cross-head speed of 0.5 mm/min and full scale load of 2500 kg. Flexural strength was determined using the formula (1) [Chen et al., 2006].

$$\sigma_f = \frac{3P_f L}{2bh^2} \tag{1}$$

where P_f is the load at which specimen being fractured, L is the length of over which the load is applied, b is the width and h is height of sample.

Polished bioactive glass-ceramic samples and using the hardness testing machine, the size of sample was 10 mm × 10 mm × 10 mm according to ASTM Standard: C730-98. The indentations have been made for loads ranging between 30 mN and 2000 mN, applied at a velocity of 1 mm/s and allowed to equilibrate for 16 s before measurement. Micro hardness, H (GPa) of 1 mm/s was calculated using the formula (2) [Michel et al., 2004].

$$H = 1.854\frac{P}{d2} \tag{2}$$

where P (N) is the applied load on sample and d (m) is the diagonal of the impression.

Compressive strength of the base glass, cobalt oxide doped bioactive glass-ceramics (2 cm × 2 cm × 1 cm size) according to ASTM D3171 were subjected to compression test. The test was performed using Instron Universal Testing Machine at room temperature (cross speed of 0.05 cm/min and full scale of 5000 kgf).

The densities of casted glass-ceramic were measured by Archimedes principle with water as the immersion fluid. The measurements were performed at room temperature. All the weight measurements have been made using a digital balance (Sartorius Model: BP221S, USA) having an accuracy of ±0.0001 g. Density (ρ) of sample was obtained by employing the relation as given below in Eq. (3).

$$\text{Density} = \frac{M_a}{M_a - M_i} \times 0.988 \tag{3}$$

where M_a (weight of sample in air) and M_i (weight of sample in water) glass-ceramic samples.

pH measurement and SEM bioactive glass-ceramic samples

2.0 g of the powdered glass-ceramic sample was soaked in 20 ml of SBF solution at 37 °C for different days and the pH was measured using microprocessor based pH-EC meter (model-1611, ESICO-USA). The instrument was calibrated each time with standard buffer solutions of pH 4.00 and 7.00 at room temperature and pH values were recorded after different time periods at a fixed interval. The glass powders (2 g) were pressed (load of 10 MPa) into pellet form using an evocable die to produce discs of 10 mm in dia for SEM analysis of bioactive glass samples. The pellets were immersed in SBF (20 ml) for 15 days at 37 °C and the surface morphology of samples was analyzed before and after SBF treatment using a scanning electron microscope (SEM – Inspect S50, FEI). The samples were coated with gold (Au) by sputter coating instrument before analyzing by SEM.

Isolation and culture of the osteoblast cells

Normal rabbits with the age group 18–24 months having average weight of 1.5–2.5 kg were operated in the Department of Orthopedics, Institute of Medical Science (Banaras Hindu University), Varanasi, India after the study was approved by the Ethical Committee of the Department of Orthopedics, IMS, BHU, Varanasi under aseptic conditions. Bone is present in particularly in iliac bone. Bone was harvested from the iliac bone of the rabbit by creating the defect of 3–4 mm. The tissues were washed with phosphate saline buffer. Bone tissues were minced into small pieces using tissue homogenizer and small pieces of the tissue were again washed thoroughly with phosphate saline buffer (Himedia, Mumbai, India). The enzymes (trypsin (Himedia, Mumbai, India) and collagenase type I (Himedia, Mumbai, India)) were dissolved in Dulbecco's Modified Eagle's Medium (DMEM, Low Glucose (Himedia, Mumbai, India)) supplemented with 1% antibiotic and antimycotic solution (Himedia, Mumbai, India). Tissue was subjected to sequential enzymatic digestion. The first digestion was done with trypsin in shaking flask at humidified 5% CO_2 environment. After trypsin digestion, tissue was washed thrice with DMEM media supplemented with the 10% Fetus bovine serum (FBS) (Himedia, Mumbai, India). After trypsin action, bone tissue was treated with the collagenase for overnight treatment in at 5% CO_2 in a humidified environment. After complete digestion, the solution was filtered through 70 μm sterile nylon mesh and the filtrate was subjected to centrifugation at 3500 rpm for 20 min. After centrifugation supernatant was discarded and cell pellet was dissolved in DMEM media. Further, the cells were seeded on the powder having a concentration of 2 × 106 cells per ml by static method.

In vitro cytotoxicity and cell proliferation assay

The osteoblast cells directly seeded to the above mentioned materials (glass-ceramic) in powder form. The experiment was performed to influence the evaluation of the cytotoxicity of the bioactive glass-ceramic samples. The analysis was performed according to the previous literature by the neutral red uptake methodology [29–32]. Proliferation assay of the cell seeded glass-ceramic materials was performed using MTT (3-(4,5-dimethylthiazol-2-y1)-2,5-diphenyltetrazolium bromide assay (Himedia, Mumbai, India) Assay. In short, MTT assay measures mitochondrial dehydrogenase activity of the viable cell. Briefly, 10 μL of MTT solution (5 mg/mL) was added to the cultured osteoblast and 24 well plate was incubated at 37 °C for different time periods. Dimethyl sulfoxide (DMSO) (Himedia, Mumbai, India) of 100 μL was used to solubilize formazan and absorbance was measured at 590 nm in a microplate reader (2030 multi label reader Victor X3, Perklin Elmer, USA) [33].

Results and discussion

Differential thermal analysis (DTA) of bioactive glasses

The differential thermal analysis (DTA) plots of base and bioactive glasses are shown in Fig. 1. It is observed that the decrease endothermic as well as exothermic peaks may be due to incorporation of nickel oxide in base bioactive glass. The results demonstrated that Tg of the glass has reduced from 538 °C to 447 °C and Tc decreased from 727 °C to 609 °C in the nickel oxide doped bioactive glass with reference to 45S5 glass. Further a decrease in the glass transition temperature (Tg) in DTA curves (Fig. 1) with increasing addition of NiO up to 2.0 mol% in a concentration dependent manner had shown that Ni^{2+} ion acted as an intermediate in smaller quantities. The present

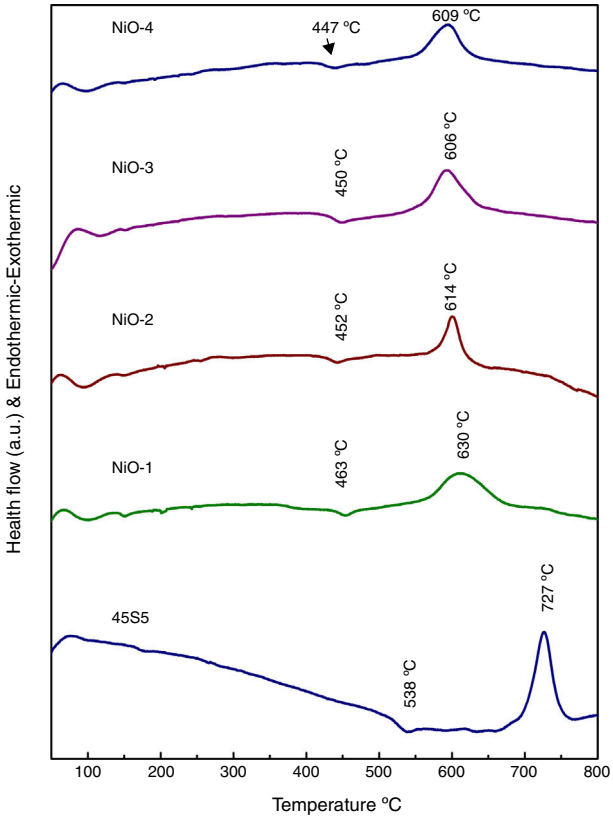

Fig. 1 – DTA of the bioactive glass samples.

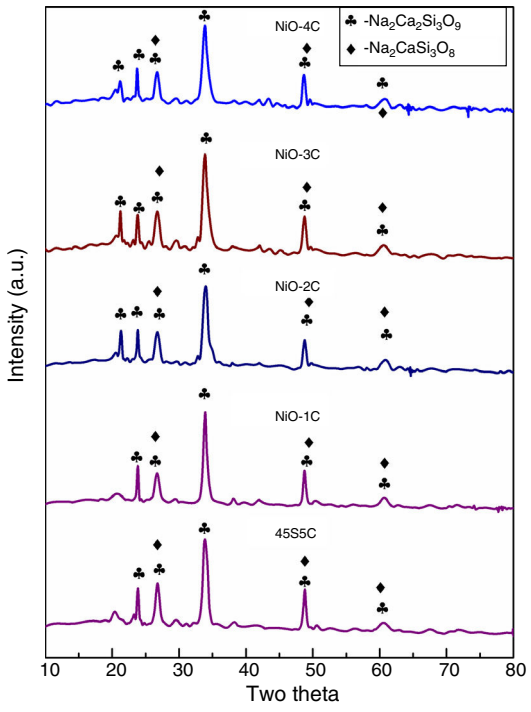

Fig. 2 – XRD of the bioactive glass-ceramics samples.

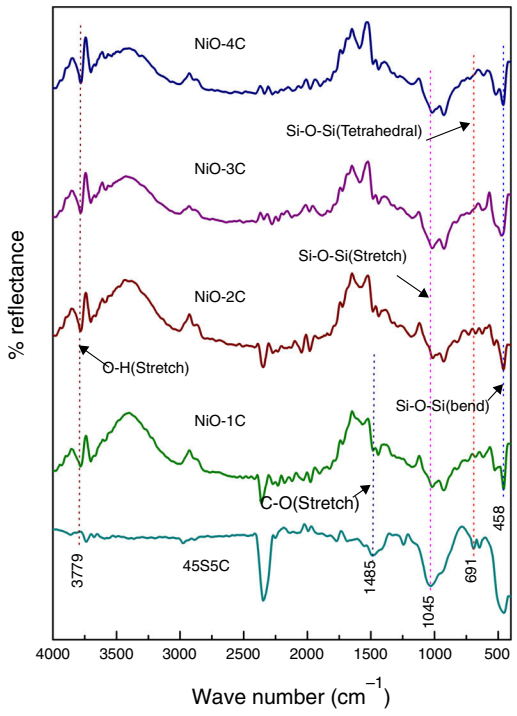

Fig. 3 – FTIR of the bioactive glass-ceramic samples.

trend of decrease in Tg with increasing concentration of NiO up to 1.65 mol% in our bioglass samples are well supported with earlier observations made by Azevedo et al. [26] for their bioactive glasses who mentioned that a decrease in glass transition temperature determined by differential scanning calorimetry (DSC) had shown that addition of CoO in smaller amounts up to 2.0 mol% acted as an intermediate and further addition up to 4.0 mol% CoO in larger quantities had acted as a modifier in the glass.

X-ray diffraction (XRD) patterns of bioactive glass-ceramic

The X-ray diffraction (XRD) patterns for base glass-ceramic and nickel oxide doped bioactive glass-ceramic are shown in Fig. 2. The XRD patterns of all the glass-ceramic substitute and un-substitute show the presence of crystalline phase of sodium calcium silicate [$Na_2Ca_2Si_3O_9$](card no: PDF#01-10782 PDF#02-0961, $Na_2CaSi_3O_8$(card number: PDF#12-0671). So, in the XRD result nickel oxide substitute and un-substitute glass-ceramics did not contain Ni as separate crystalline phase. This can be related to their relatively low contents in bioactive glass composition. The past studies on sintered 45S5 bioactive glass and doped oxide glasses had also shown the same crystalline phase [34].

FTIR reflection spectra of bioactive glass-ceramic

Fig. 3 shows the FTIR reflection spectra of bioactive glass-ceramic substituted with nickel oxide before SBF treatment and in the base glass-ceramic the peaks were found at 458, 691, 1045, 1485 and 3779 cm^{-1}. FTIR reflection spectral bands of bioactive glass-ceramics have confirmed the main characteristics of silicate network and this may be attributed due to the presence of SiO_4 as a major functional group. The resultant FTIR band at 458 cm^{-1} is associated with a Si–O–Si symmetric bending mode, the band at 691 cm^{-1} corresponds with Si–O–Si symmetric stretch of non-bridging oxygen atoms between silicate tetrahedra. The major band at about 1045 cm^{-1} can be attributed to Si–O–Si stretching mode of vibration. The small band at 1485 cm^{-1} has been attributed to C–O vibration mode. The small broad band centered at about 3779 cm^{-1} can be assigned to hydroxyl group (–OH) or adsorbed water molecules [27]. The bioactive glass-ceramics substituted with nickel oxide has not shown any noticeable change in the FTIR spectral bands position.

In vitro bioactivity of bioactive glass-ceramic by FTIR spectrometry

Figs. 4–8 show the FTIR reflectance spectral bands of the bioactive glass-ceramic before and after immersion in SBF for different days such as 0, 1, 3, 7, 15 and 30 days. Hench [35], Kim et al. [36] and Rehman et al. [37] demonstrated the changes in the FTIR spectral bands after immersion in SBF and the stages of apatite formation on the surface of the samples after immersion in SBF.

Fig. 4 shows the FTIR bands of 45S5C sample before and after treated with SBF. The new bands appeared after 1 day of immersion in SBF when compared before immersion at 534 and 612 cm^{-1} which correspond to P–O bending (crystalline) and P–O bending (amorphous), respectively. The presence of C–O stretching 927 cm^{-1} bonds shows the crystalline nature which indicates the formation of hydroxyl carbonate apatite (HCA) layer. The bands at about 1430 and 1588 cm^{-1} are associated with C–O (stretch) and C=O (stretch) stretching mode and the band at about 3807 cm^{-1} can be assigned due to (hydroxyl)

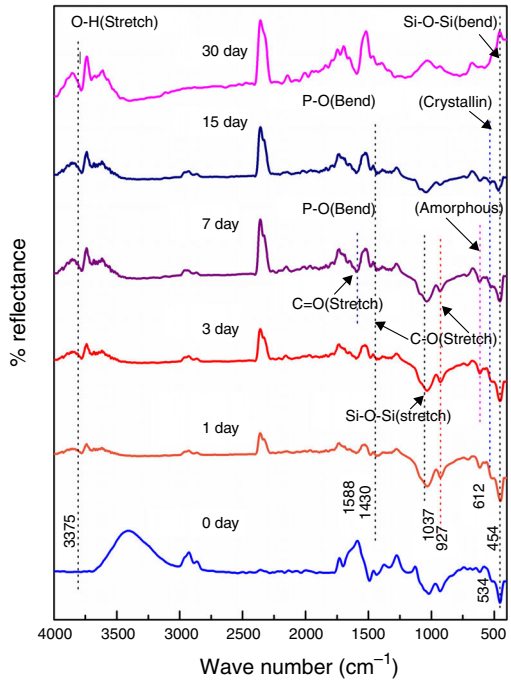

Fig. 4 – FTIR of the bioactive glass-ceramic (45S5 bioglass-ceramic) before and after immersion in SBF for different days.

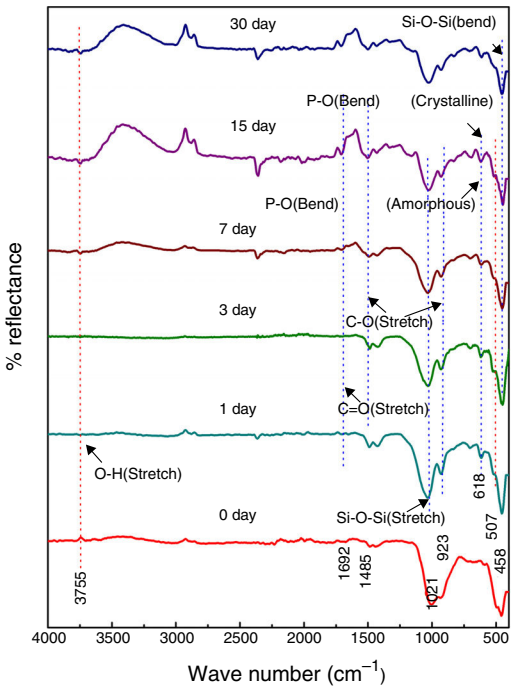

Fig. 5 – FTIR of the bioactive glass-ceramic (NiO-1C) before and after immersion in SBF for different days.

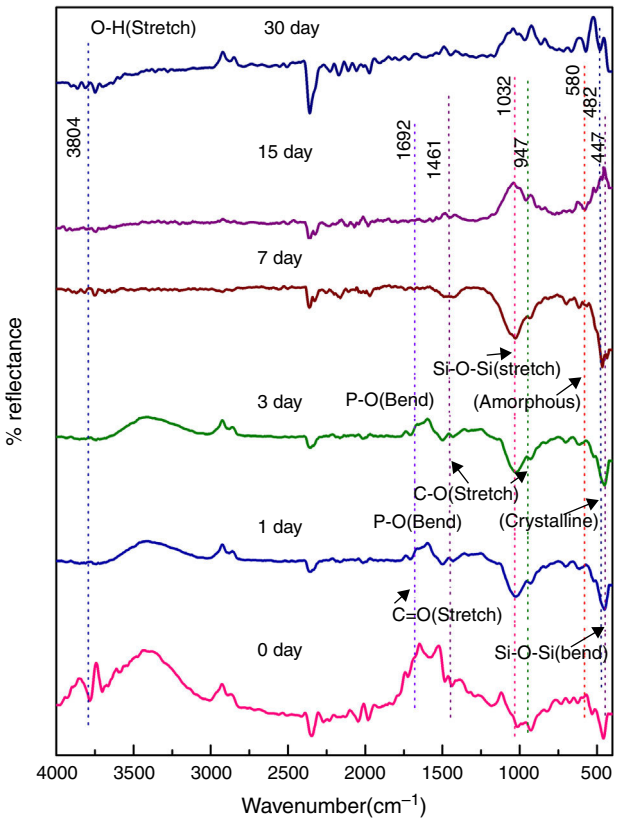

Fig. 6 – FTIR of the bioactive glass-ceramic (NiO-2C) before and after immersion in SBF for different days.

O–H groups on the surface of the samples. The prolonged time periods of the samples in SBF show the same behavior with a small decrease in the intensities of the bands, which resulted in favor of the formation of hydroxyl carbonated apatite (HCA) layer.

Fig. 5 shows the FTIR bands of NiO-1C sample before and after treated with SBF. The new bands were appeared after 1 day immersion in SBF when compared to before immersion at 507 and 618 cm^{-1} which corresponds to P–O bending (crystalline) and P–O bending (amorphous) respectively. The presences of C–O stretching 923 cm^{-1} bonds show the crystalline nature which indicates the formation of hydroxyl carbonate apatite (HCA) layer. The bands at about 1485 and 1692 cm^{-1} are associated with C–O (stretch) and C=O (stretch) stretching mode and the band at about 3755 cm^{-1} can be assigned due to (hydroxyl) O–H groups on the surface of the samples. The prolonged period of the samples in SBF shows the same behavior with a small decrease in the intensities of the bands, which are resulted in favor of formation of hydroxyl carbonated apatite (HCA) layer.

Fig. 6 shows the FTIR bands of NiO-2C sample before and after treated with SBF. The new bands were appeared after 1 day immersion in SBF when compared to before immersion at 482 and 580 cm^{-1} which corresponds to P–O bending (crystalline) and P–O bending (amorphous) respectively. The presence of C–O stretching 947 cm^{-1} bond show the crystalline nature which indicates the formation of hydroxyl carbonate apatite (HCA) layer. The bands at about 1461 and 1692 cm^{-1}

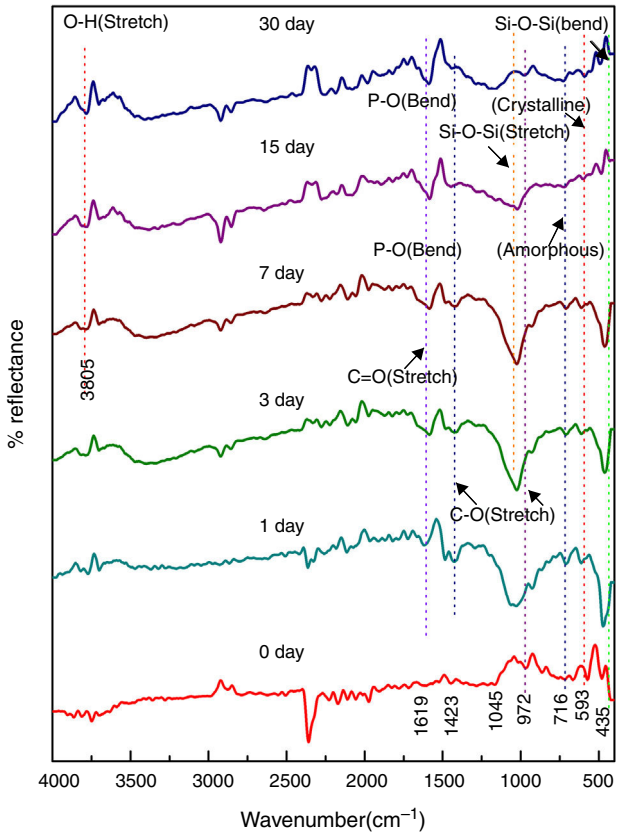

Fig. 7 – FTIR of the bioactive glass-ceramic (NiO-3C) before and after immersion in SBF for different days.

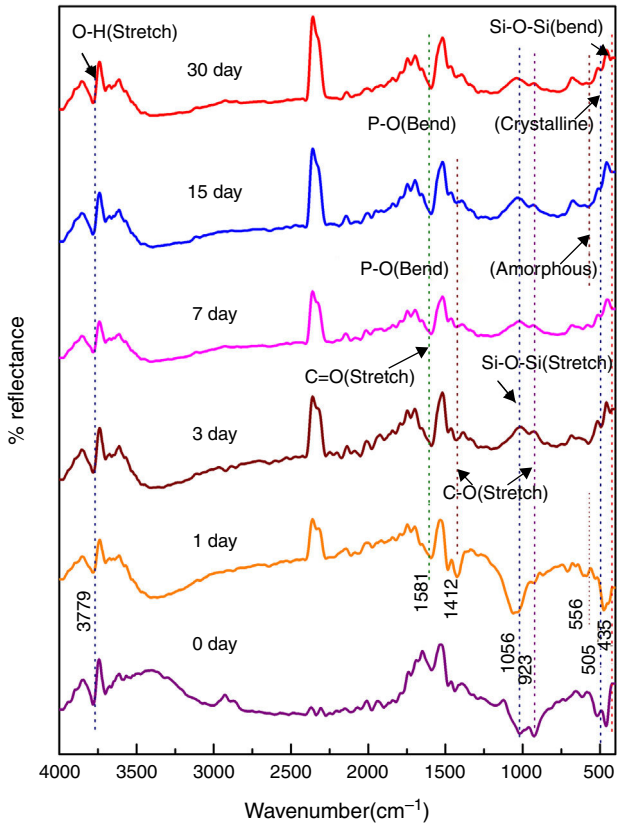

Fig. 8 – FTIR of the bioactive glass-ceramic (NiO-4C) before and after immersion in SBF for different days.

are associated with C–O (stretch) and C=O (stretch) stretching mode and the band at about 3804 cm^{-1} can be assigned due to (hydroxyl) O–H groups of the samples. The prolonged period of the samples in SBF shows the same behavior with a small decrease in the intensities of the bands, which are resulted in favor of formation of hydroxyl carbonated apatite (HCA) layer.

Fig. 7 shows the FTIR bands of NiO-3C sample before and after treated with SBF. The new bands were appeared after 1 day immersion in SBF when compared to before immersion at 593 and 716 cm^{-1} which corresponds to P–O bending (crystalline) and P–O bending (amorphous) respectively. The presence of C–O stretching 972 cm^{-1} band show the crystalline nature which indicates the formation of hydroxyl carbonate apatite (HCA) layer. The bands at about 1423 and 1691 cm^{-1} are associated with C–O (stretch) and C=O (stretch) stretching mode and the band at about 3805 cm^{-1} can be assigned due to (hydroxyl) O–H groups on the surface of the samples. The prolonged period of the samples in SBF shows the same behavior with a small decrease in the intensities of the bands, which are resulted in favor of formation of hydroxyl carbonated apatite (HCA) layer.

Fig. 8 shows the FTIR bands of NiO-4C sample before and after treated with SBF. The new bands were appeared after 1 day immersion in SBF when compared to before immersion at 505 and 556 cm^{-1} which corresponds to P–O bending (crystalline) and P–O bending (amorphous) respectively. The presence of C–O stretching 923 cm^{-1} band show the crystalline nature which indicates the formation of hydroxyl carbonate apatite (HCA) layer. The bands at about 1412 and 1581 cm^{-1} are associated with C–O (stretch) and C=O (stretch) stretching mode and the band at about 3779 cm^{-1} can be assigned due to (hydroxyl) O–H groups on the surface of the samples. The prolonged period of the samples in SBF shows the same behavior with a small decrease in the intensities of the bands, which are resulted in favor of formation of hydroxyl carbonated apatite (HCA) layer.

Mechanical properties and density measurements

Fig. 9 shows the results of the flexural strength and micro hardness for 45S5C, NiO-1C, NiO-2C, NiO-3C and NiO-4C samples. The results demonstrate an increasing tendency in flexural strength and micro hardness as the percentage of nickel oxide (103, 107, 109, 113 and 120 MPa) and (7.68, 7.81, 7.86, 8.09 and 8.14 GPa) increased, respectively. This can be easily understood that more the flexural strength and micro hardness of base glass-ceramic and bioactive glass-ceramic substitute with nickel oxide, the more would be the compactness of glass structure [33]. Fig. 10 shows the results of the density and compressive strength for 45S5C, NiO-1C, NiO-2C, NiO-3C and NiO-4C samples. The results demonstrate an increasing tendency in density and compressive strength with increasing percentage of the nickel oxide (2.82, 2.94, 2.95, 2.97 and 2.99 g/cm^3) and (113, 118, 121, 126 and 132 MPa), respectively. This is attributed due to the reason that lighter element

silicon has been replaced by heavier element nickel up by limited substitution of NiO from 0 to 1.65 mol% in the bioactive glass samples. The results show that more the flexural strength and micro hardness of base glass-ceramic and bioactive glass-ceramic substituted nickel oxide, the more would be the compactness of the structure of the glass [24,38].

By isotopic and isomorphic substitution of nickel, Smith et al. [25] had shown that there were no appreciable difference in structural co-relation between 45S5 bioglass and NiO doped bioactive glass which indicated that addition of Ni^{2+} ion would not adversely affect the overall bioactivity and structure of the glass. The Ni^{2+} (0.58 Å) such as Co^{2+} (0.55 Å) and Mg^{2+} (0.57 Å) ions has similar ionic radii and cationic charge state, respectively [28]. Because of the similar ionic radii and therefore similar charge to size ratio, it might be expected that Ni^{2+} would adopt similar structural role as Co^{2+} and Mg^{2+} ions which had been shown earlier to act as a network intermediate [25]. It is mentioned herewith that due to charge/size ratio of Ni^{2+} ion, it would enter into $[SiO_4]^{4-}$ network as $[NiO_4]^{2-}$ species in tetrahedral coordination but it could also act as network modifier in higher coordination. Azevedo et al. [26] had

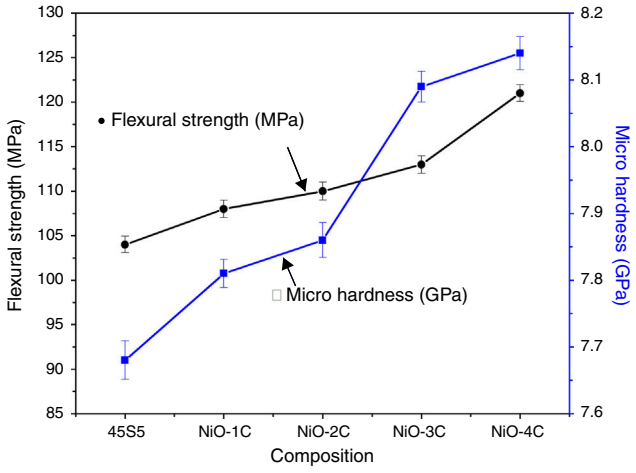

Fig. 9 – Flexural strength and micro hardness of the bioactive glass-ceramic samples.

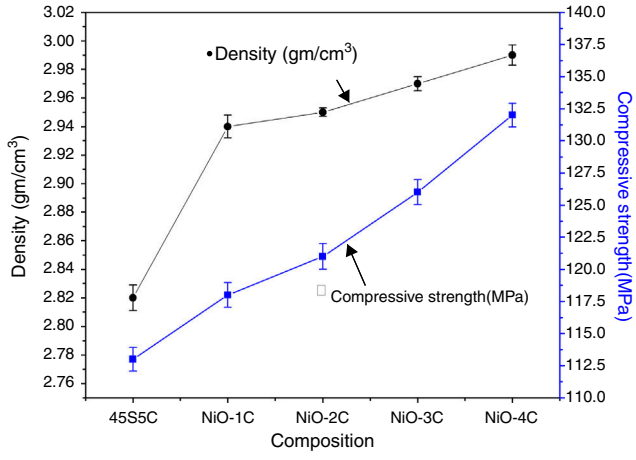

Fig. 10 – Density and compressive strength of the bioactive glass-ceramic samples.

also made similar observation with cobalt that due to same charge/ratio of Co^{2+} ion, it would enter into silicate $[SiO_4]^{4-}$ network as $[CoO_4]^{2-}$ complex ion in tetrahedral coordination but it would act as modifier in higher coordination. The role of nickel oxide in the bioglass would determine the connectivity (NC) and the bioglass properties such as ion release rates and its effect on hydroxyl carbonate apatite formation. Smith et al. [25] studied the structural characterization of hypoxia-mimicking bioactive glasses containing up to 4 mol% NiO by isotopic and isomorphic substitution using neutron diffraction method and reported the Ni–O–Si bonding in silicate network with one third (~33%) of Ni^{2+} ion occupying a network forming tetrahedral geometry and its two-third (~67%) occupying a 5-fold environment in the bioglass. In the diffraction pattern, the main feature at around (2 Å) corresponded to the nearest of Ni–O co-relations. The co-relation at around (2 Å) was attributed partially due to 4-fold Ni–O and 5-fold Ni–O where there are 4 short bonds of (1.98 Å) and one longer bond at (2.19 Å). The authors found that there was an excellent agreement between metal-oxygen (M–O) correlation obtained for Ni by isotopic substitution and Ni/Co data sets by isomorphic substitution method which confirmed that both Ni^{2+} and Co^{2+} ion were isostructural in the bioactive glasses. The entry of heavier Ni^{2+} ion as $[NiO_4]^{2-}$ tetrahedral species in place of lighter Si^{4+} ion in $[SiO_4]^{4-}$ network has resulted the formation of Ni–O–Si bonds in silicate network structure as such the mechanical properties and densities of the bioactive glass-ceramics samples have increased considerably with increasing NiO concentration. Vyas et al. [4,39,40] in an earlier investigation had also shown that the addition of cobalt oxide up to 2.0 wt% in 45S5 bioactive glass-ceramic has resulted in an increase in density and compressive strength of their samples due to formation Co–O–Si bonds.

Azevedo et al. [26] had also performed the ^{29}Si MAS-NMR to determine the role of Co^{2+} ion in the silicate glass structure and reported the dual role of Co^{2+} as an intermediate and modifier in their bioglass samples depending upon its concentration like Mg^{2+}, Ca^{2+} and Zn^{2+} ions. Although the effect of doping of NiO for SiO_2 has not been investigated presently in the glass samples by NMR spectroscopy however, further investigation on doping of NiO in silicate glass network by NMR would be very interesting in determining the network connectivity and bioactivity of the glasses in future.

Singh et al. [41] had also reported previously the change in band intensity which resulted a change in color shades produced by Ni^{2+} ion from light yellow to brownish to violet due to change in nickel ion coordination as Li_2O was replaced by Na_2O and Na_2O was replaced by K_2O in binary alkali silicate glass. The small concentration of nickel oxide was doped in the alkali silicate ($30R_2O{\cdot}70SiO_2$ where $R^+ = Li^+, Na^+$ and K^+ ion) glass of constant composition up to 0.5 wt% of NiO. Since the coordination of Ni^{2+} ion is dependent upon the nature of alkali oxides in the glass as such the authors mentioned that the main absorption band due to Ni^{2+} ion centered at λ_{max} around 440 nm in lithium silicate was associated predominantly with octahedral symmetry where as the band at 455 nm in sodium silicate glass was associated with a mixture of octahedral and tetrahedral symmetries. However, in potassium silicate glass the visible absorption band due to Ni^{2+} ion centered at

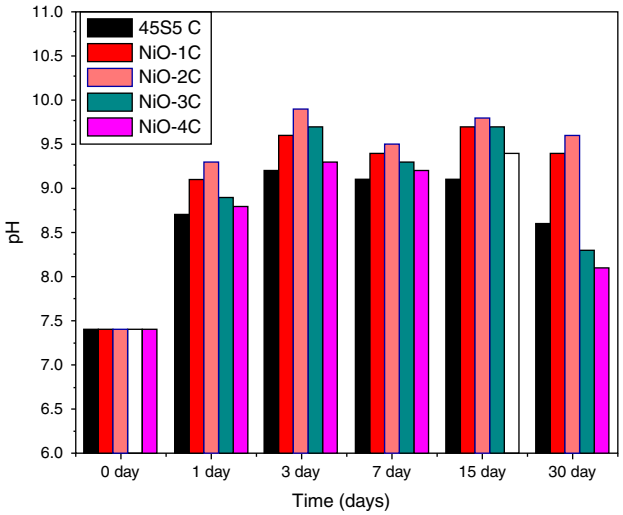

Fig. 11 – pH behavior of the SBF after immersion of the bioactive glass-ceramic samples.

around 550 nm was mainly due to tetrahedral symmetry in the glass.

pH behavior in SBF

The variation in pH values of simulated body fluid (SBF) after soaking the base glass-ceramic and bioactive glass-ceramic for various time periods is shown in Fig. 11, respectively. It was observed that due to substitution of nickel oxide in the base bioactive glass-ceramic (45S5C) the pH values of SBF solution increased during first 3 days of soaking because of faster release of Ca^{2+} and Na^{+} ions from the sample surface caused by an increase in the pH value. Then it is found to decrease and attain nearly a constant value in all the cases. The reactions occurred in favor of formation of hydroxyl carbonate apatite like layer on the surface of the samples [4,35].

Scanning electron microscopy (SEM) analysis of glass-ceramic samples

The SEM micrographs of base glass and nickel oxide substituted glass samples before immersion in SBF solution are shown in Fig. 12 which shows different rod types of structure and asymmetrical grain of bioactive glass-ceramic samples. It is quite similar to result reported by Hanan et al. [33]. Fig. 13 represents the SEM micrographs of base glass-ceramic and nickel oxide substituted bioactive glass-ceramic after immersion in SBF for 15 days. It is clearly understood from the Fig. 13 that base glass-ceramic and nickel substituted glass-ceramic samples immersed in SBF solution for 15 days were enclosed with asymmetrical shape and grounded carbonated-HA particles have grown into more than a few agglomerates consisting of spine shaped HCA layer. These micrographs show the formation of HCA on the surface of base and NiO substituted bioactive glass-ceramic samples after immersion in SBF solution for 15 days [34,36].

In vitro cytotoxicity and cell proliferation assay

The cytotoxicity is one of the biological evaluation and screening test to find out the cell viability and to check

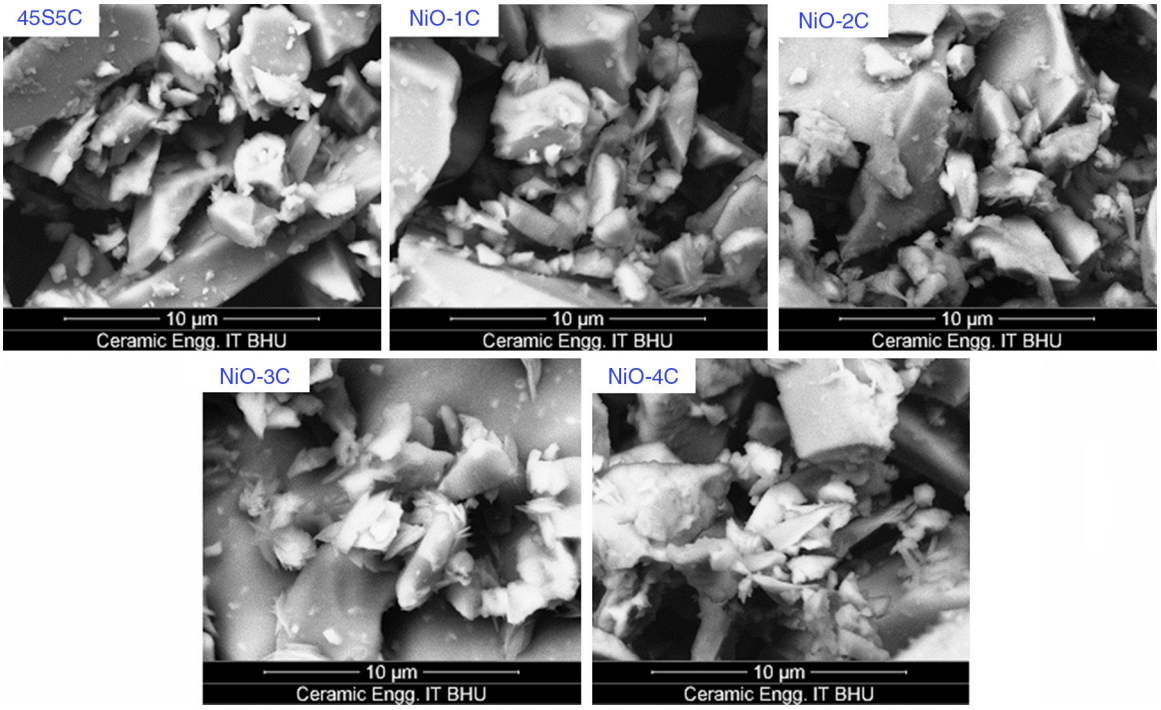

Fig. 12 – Scanning electron microscope (SEM) of glass-ceramic samples before SBF.

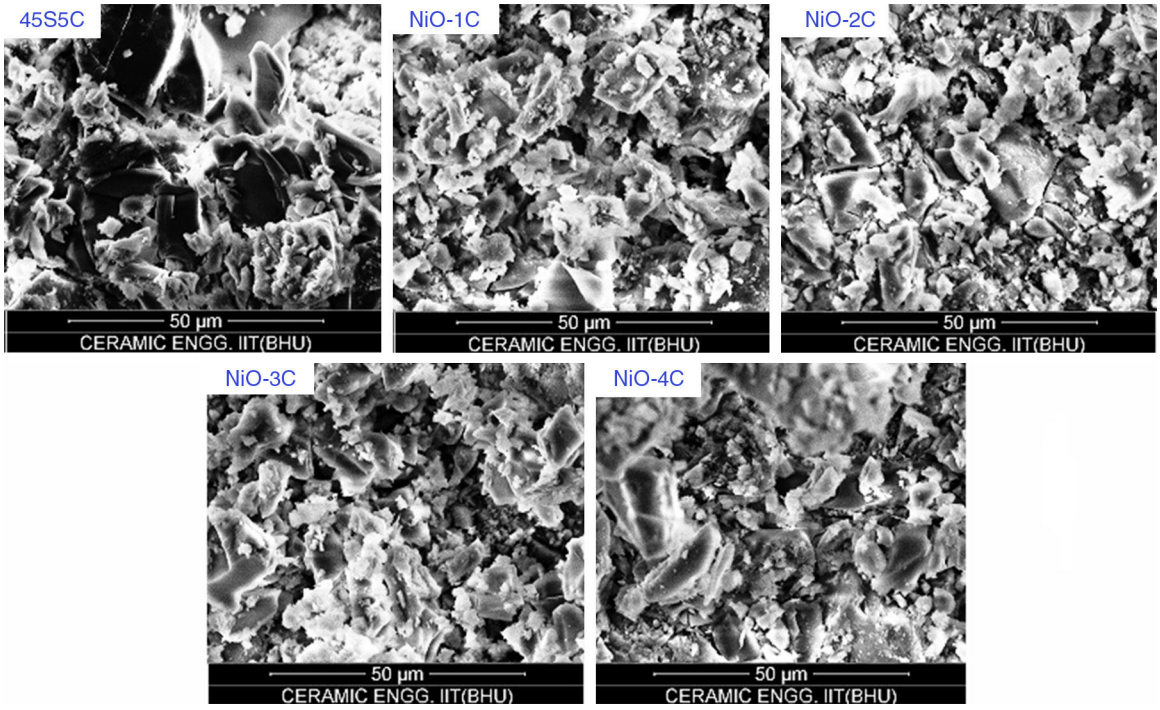

Fig. 13 – Scanning electron microscope (SEM) of glass-ceramic samples after SBF.

whether it is biocompatible. The test was carried out in osteoblast cells for each concentration and repeated thrice times to make sure that variables such as cell population in the solutions did not introduce any systematic mistake. The given below graph shows the amount of cell viable after performing the experiment. The value shows more similar to or exactly 80% (Fig. 14a). For the primary cell culture more than 80% cell viability used for the better metabolic activity and cell proliferation. The cell proliferation assay results show (Fig. 14b) that the free osteoblast cells decrease its viability after 3, 5, 7 days of culture. The result shows that the cell proliferation rate was highest in the sample NiO-2C which exactly matches the result with cytotoxicity test. From the study it was clarified that the above mentioned glass-ceramic material can be used for the in vivo study.

Conclusions

In the present investigation, a comparative investigation was made on physico-mechanical and bioactive properties of nickel oxide substitute 45S5 bioactive glass-ceramics. The following conclusions were drawn from this study. It is concluded that an increase in nickel oxide content in this series of glass-ceramic resulted in an increase in bioactivity. This is also supported by pH and SEM analysis. FTIR results showed the silicate network structure in prepared bioactive glass-ceramic. Further, an increase in the nickel oxide content in 45S5 bioactive glass-ceramic increases the density, micro hardness, flexural strength due to formation of Ni–O–Si bonds in silicate network structure to and the main

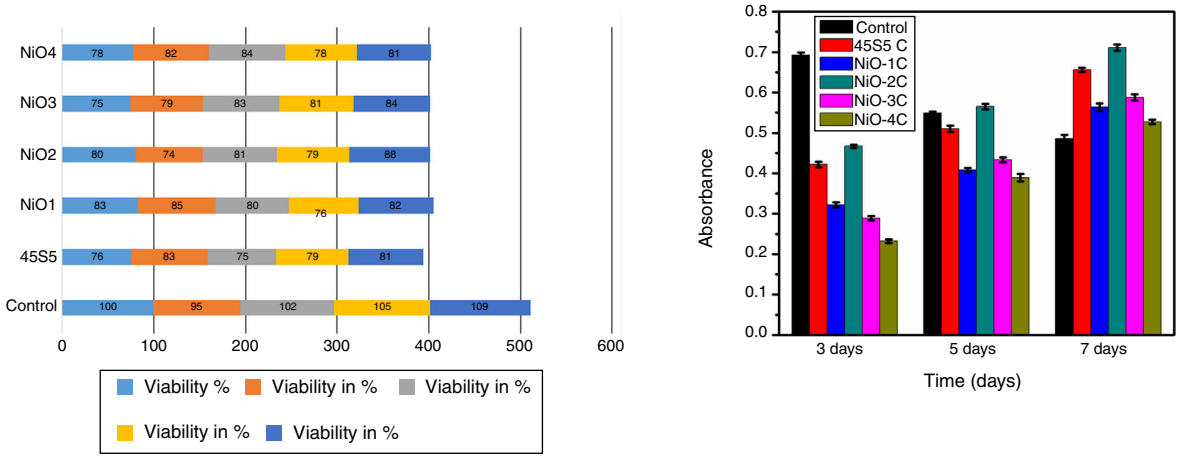

Fig. 14 – (a) Cytotoxicity analysis, and (b) proliferation assay of cells on glass-ceramic samples at 3rd, 5th and 7th days of culture.

crystalline phases is sodium calcium silicate [Na_2Ca_2 Si_3O_9 and $Na_2CaSi_3O_8$]. The cell culture studies have shown that the bioactive glass ceramic samples containing small concentration of NiO from 0 to 1.65 mol% were non cytotoxic against osteoblast cells. The cell proliferation rate was highest in the sample no NiO-2C which was found to match exactly with the result of cytotoxicity test. Hence, the present investigation clearly concluded that NiO doped bioactive glass-ceramics would be potential biomaterials for biomedical applications.

Acknowledgements

The authors gratefully acknowledge the HOD Department of Ceramic Engineering, Indian Institute of Technology (Banaras Hindu University) Varanasi 221005, India and the honorable Director, IIT (BHU) Varanasi, India for providing necessary facilities for the present work. The author, Vikas Kumar Vyas is also very much grateful to the University Grants Commission, New Delhi, India for providing the Rajiv Gandhi National Fellowship (RGNF-SC-UTT-2012-13-25709) for this research work.

REFERENCES

[1] L.L. Hench, R.J. Splinter, W.C. Allen, T.K. Greenlee, Bonding mechanisms at the interface of ceramic prosthetic materials, J. Biomed. Mater. Res. Symp. 5 (1971) 25.
[2] A.E. Clark, L.L. Hench, H.A. Paschall, Influence of surface chemistry on implant interface histology—theoretical basis for implant materials selection, J. Biomed. Mater. Res. 10 (1976) 161–174.
[3] P. Sepulveda, J.R. Jones, L.L. Hench, Characterization of melt-derived 45S5 and sol–gel-derived 58S bioactive glasses, J. Biomed. Mater. Res. 58 (2001) 734–740.
[4] Arepalli Sampath Kumar, Tripathi Himanshu, Vikash Kumar Vyas, Jain Shubham, Suman Shyam Kumar, Ram Pyare, S.P. Singh, Mater. Sci. Eng. C 49 (2015) 549–559.
[5] Julian R. Jones, Review of bioactive glass: from Hench to hybrids, Acta Biomater. 9 (2013) 4457–4486.
[6] M.N. Rahaman, D.E. Day, B.S. Bal, Q. Fu, S.B. Jung, L.F. Bonewald, A.P. Tomsia, Bioactive glass in tissue engineering, Acta Biomater. 7 (2011) 2355–2373.
[7] L.L. Hench, O. Andersson, in: L.L. Hench, J. Wilson (Eds.), An Introduction to Bioceramics, World Scientific, Singapore, 1993, p. 41.
[8] A. Ito, K. Ojima, H. James, G.W. Hastings, J.C. Knowles, I. Olsen, J. Mater. Sci. Mater. Med. 11 (2000) 615.
[9] H. Kawamura, A. Ito, S. Miyakawa, P. Layrolle, K. Ojima, N. Incinose, T. Tateishi, J. Mater. Sci. Mater. Med. 50 (2000) 184.
[10] A. Kesisoglou, J.C. Knowles, I. Olsen, J. Mater. Sci. Mater. Med. 13 (2002) 1189.
[11] F.H. ElBatal, A. ElKheshen, Mater. Chem. Phys. 110 (2–3) (2008) 352–362.
[12] S. Kumar, P. Vinatier, A. Levasseur, K.J. Rao, Solid State Chem. 177 (4–5) (2004) 1723–1737.
[13] A. Oki, B. Parveen, S. Hossain, S. Adeniji, H. Donahue, J. Biomed. Mater. Res. A69 (2) (2004) 216–221.
[14] A. Saboori, M. Sheikhi, F. Moztarzadeh, M. Rabiee, S. Hesaraki, M. Tahriri, N. Nezafati, Adv. Appl. Ceram. 108 (3) (2009) 155–161.
[15] T. Kasuga, Y. Abe, J. Non-Cryst. Solids 243 (70) (1999).
[16] T. Kasuga, M. Sawada, M. Nogami, Y. Abe, Biomaterials 20 (1999) 1415.
[17] L.L. Hench, I. Thompson, J. R. Soc. Interface 7 (2010) 379–391.
[18] S. Jung, Missouri University of Science and Technology (PhD dissertation), 2010.
[19] J.R. Jones, L.M. Ehrenfried, P. Saravanapavan, L.L. Hench, J. Mater. Sci. Mater. Med. 17 (2006) 989–996.
[20] M. Diba, F. Tapia, A.R. Boccaccini, Int. J. Appl. Glass Sci. 3 (2012) 221–253.
[21] Aylin M. Deliormanlı, J. Mater. Sci. Mater. Med. 26 (2015) 67.
[22] L.L. Hench, J.M. Polak, Science 295 (2002) 1014.
[23] A.V. Gayathri Devi, V. Rajendran, N. Rajendran, Mater. Chem. Phys. 124 (2010) 312–318.
[24] Alexander Hoppe, Bojan Jokic, Djordje Janackovic, Tobias Fey, Peter Greil, Stefan Romeis, Jochen Schmidt, Wolfgang Peukert, Jonathan Lao, Edouard Jallot, Aldo R. Boccaccini, ACS Appl. Mater. Interfaces 6 (2014) 2865–2877.
[25] Jodie M. Smith, Richard A. Martin, Gabriel J. Cuelloc, Robert J. Newporta, J. Mater. Chem. B 1 (2013) 1296–1303.
[26] M.M. Azevedo, G. Jell, M.D. O'Donnell, R.V. Law, R.G. Hill, M.M. Stevens, J. Mater. Chem. 20 (2010) 8854–8864.
[27] C. Wu, Y. Zhou, W. Fan, P. Han, J. Chang, J. Yuen, M. Zhang, Y. Xiao, Biomaterials 33 (2012) 2076–2085.
[28] T. Kokubo, H. Takadama, Biomaterials 27 (2006) 2907–2915.
[29] ISO 10993-5, Biological Evaluation of Medical Devices. Part 1: Guidance on Selection of Tests, International Organization for Standardization, 2009.
[30] L.C. Keong, A.S. Halim, In vitro models in biocompatibility assessment for biomedical-grade chitosan derivatives in wound management, Int. J. Mol. Sci. 10 (3) (2009) 1300–1313.
[31] G. Thrivikraman, G. Madras, et al., In vitro/in vivo assessment and mechanisms of toxicity of bioceramic materials and its wear particulates, RSC Adv. 4 (25) (2014) 12763–12781.
[32] J. Daguano, K. Strecker, et al., Effect of partial crystallization on the mechanical properties and cytotoxicity of bioactive glass from the 3CaO, P_2O_5–SiO_2–MgO system, J. Mech. Behav. Biomed. Mater. 14 (2012) 78–88.
[33] N. Siddiqui, K. Pramanik, Development of fibrin conjugated chitosan/nano β-TCP composite scaffolds with improved cell supportive property for bone tissue regeneration, J. Appl. Polym. Sci. 132 (9) (2015).
[34] A.K. Srivastava, R. Pyare, S.P. Singh, Int. J. Sci. Eng. Res. 3 (2012) 1–15.
[35] L.L. Hench, J. Am. Ceram. Soc. 81 (1998) 1705–1728.
[36] Tadashi Kokubo, Hyun-Min Kim, Masakazu Kawashita, Biomaterials 24 (2003) 2161–2175.
[37] I. Rehman, M. Karsh, L.L. Hench, W. Bonfield, J. Biomed. Mater. Res. 50 (May (2)) (2000) 97–100.
[38] Hanan H. Beherei, Khaled R. Mohamed, Gehan T. El-Bassyouni, Ceram. Int. 35 (2009) 1991–1997.
[39] V.K. Vyas, Arepalli Sampath Kumar, S. Prasad, S.P. Singh, Ram Pyare, Bull. Mater. Sci. Indian Acad. Sci. 38 (August (4)) (2015) 957–964.
[40] Vikash K. Vyas, Arepalli S. Kumar, Sunil Prasad, Mohammad Ershad, Saryoo P. Singh, Ram Pyare, Innov. Corros. Mater. Sci. 5 (2015) 86–92.
[41] R.S. Singh, S.P. Singh, Phys. Chem. Glas. 39 (June (3)) (1998) 140–144.